

Evidence for extra radiation? Profile likelihood versus Bayesian posterior

Jan Hamann

Department of Physics and Astronomy
University of Aarhus, DK-8000 Aarhus C, Denmark

E-mail: hamann@phys.au.dk

Abstract. A number of recent analyses of cosmological data have reported hints for the presence of extra radiation beyond the standard model expectation. In order to test the robustness of these claims under different methods of constructing parameter constraints, we perform a Bayesian posterior-based and a likelihood profile-based analysis of current data. We confirm the presence of a slight discrepancy between posterior- and profile-based constraints, with the marginalised posterior preferring higher values of the effective number of neutrino species N_{eff} . This can be traced back to a volume effect occurring during the marginalisation process, and we demonstrate that the effect is related to the fact that cosmic microwave background (CMB) data constrain N_{eff} only indirectly via the redshift of matter-radiation equality. Once present CMB data are combined with external information about, e.g., the Hubble parameter, the difference between the methods becomes small compared to the uncertainty of N_{eff} . We conclude that the preference of precision cosmological data for excess radiation is “real” and not an artifact of a specific choice of credible/confidence interval construction.

Contents

1	Introduction	1
2	Analysis	1
2.1	Data sets	1
2.2	Model and priors	2
2.3	Marginalised posterior and profile likelihood	2
2.4	Construction of the profile likelihood	3
3	Results	3
4	Discussion	7
A	Profiling with Markov chains	9

1 Introduction

In the past years, measurements of the temperature and polarisation anisotropies in the cosmic microwave background have revealed a wealth of information about the Universe. One particular quantity that can be inferred from CMB data is the relativistic energy density ρ_r around decoupling, typically expressed in terms of the effective number of massless neutrino degrees of freedom N_{eff} :

$$\rho_r = \frac{\pi^2}{15} T_\gamma^4 (1 + \alpha N_{\text{eff}}), \quad (1.1)$$

where $T_\gamma = (2.72548 \pm 0.00057)$ K [1] is the CMB temperature and $\alpha \equiv \frac{7}{8} \left(\frac{4}{11}\right)^{4/3}$. The three standard model neutrino species are expected to contribute $N_{\text{eff}} = 3.046$ effective degrees of freedom [2]. Intriguingly however, present cosmological data show some indication for $N_{\text{eff}} > 3.046$ [3–9], hinting at the possible existence of further light particle species. These hints are based on a Bayesian statistics analysis of the data however, and as long as the evidence for $N_{\text{eff}} > 3.046$ is weak, one might also want to consider an alternative approach of constraining N_{eff} . A profile likelihood analysis for instance, being prior-independent and parameterisation-invariant, provides a useful cross-check of these results and is complementary to the usual Bayesian analysis based on the posterior probability density [10]. Using a profile likelihood-based analysis, it was recently claimed in [11] that the hints for $N_{\text{eff}} > 3.046$ are merely artifacts of the Bayesian construction of parameter constraints. We shall revisit this claim in the present work.

This paper is organised as follows: we will describe the details of our analysis in section 2, present our results in section 3 and conclude in section 4.

2 Analysis

2.1 Data sets

For clarity of presentation and given the considerable numerical effort required to reliably construct the profile likelihood, we will limit ourselves to two different combinations of data:

Table 1. Parameters and prior ranges for the cosmological and nuisance parameters. For each individual analysis only one out of the first three parameters is used.

Parameter	Symbol	Prior
Hubble parameter	h	0.4 \rightarrow 1.0
Dark energy density	Ω_Λ	0 \rightarrow 1
Ratio of sound horizon to angular diameter distance at decoupling	θ_s	0.5 \rightarrow 10
Baryon density	ω_b	0.005 \rightarrow 0.1
Cold dark matter density	ω_{cdm}	0.01 \rightarrow 0.99
Amplitude of scalar spectrum @ $k = 0.05 \text{ Mpc}^{-1}$	$\log[10^{10} A_s]$	2.7 \rightarrow 4
Scalar spectral index	n_s	0.5 \rightarrow 1.5
Redshift of reionisation	z_{re}	1 \rightarrow 50
Effective number of massless neutrinos	N_{eff}	1.5 \rightarrow 10
Amplitude of Sunyaev-Zel'dovich contribution	A_{SZ}	0 \rightarrow 3
Amplitude of clustered point source contribution	A_c	0 \rightarrow 20
Amplitude of Poisson point source contribution	A_P	0 \rightarrow 100

1. A CMB only set, consisting of the 7-year Wilkinson Microwave Anisotropy Probe data (WMAP7) [12] plus the 2008 Atacama Cosmology Telescope (ACT) data [13]. For this data set, the discrepancy between the Bayesian result of [13] and the profile likelihood result reported in [11] is particularly large.
2. The same data combined with a constraint on the Hubble parameter (HST) derived by Riess *et al.* [14].

2.2 Model and priors

We consider a one-parameter extension of the 6-parameter Λ CDM vanilla model, varying also the effective number of massless degrees of freedom N_{eff} on top of the standard parameters. Additionally, three parameters describing the foreground contribution to the small-scale CMB temperature spectrum are required. The parameterisation of the vanilla model is not unique, and there are a number of different choices commonly used in the literature. Since the parameterisation implicitly determines the prior probability distribution, these choices can affect the inference of parameters, even though the physical models are equivalent. In this work we explicitly compare three parameterisation choices: a flat prior on the Hubble parameter H_0 , a flat prior on the dark energy density Ω_Λ and a flat prior on the ratio of sound horizon to angular diameter distance at decoupling θ_s . We list all free parameters and their associated prior ranges in table 1. The primordial Helium fraction is fixed to $Y_p = 0.24$ in order to facilitate comparison with other authors' results.

2.3 Marginalised posterior and profile likelihood

Given a model with n free parameters, the full information of the data is contained in the n -dimensional likelihood function \mathcal{L} . If one wants to construct constraints on a single parameter φ , the dimensionality obviously needs to be reduced. Most commonly, this is done in a Bayesian framework, by first promoting \mathcal{L} to a probability density function (through multiplication with a prior probability density), and then integrating (“marginalising”) over the nuisance directions (see [10] for a more detailed discussion), resulting in the marginalised posterior. The marginalised posterior can easily be extracted from Markov chains and has

a straightforward interpretation as the probability density of the true value of φ , given the model, data and priors.

Since the choice of priors (or equivalently, the choice of parameter basis [15]) may be somewhat subjective, one might also want to consider a prior-independent construction, such as the profile likelihood \mathcal{L}^P . Here, instead of integrating over the nuisance directions, one takes the maximum value of \mathcal{L} for a fixed value of φ . Though the profile likelihood does not have a formal probabilistic interpretation, it is often used to construct approximate frequentist confidence intervals based on the likelihood ratio, by identifying the region for which $\Delta\chi_{\text{eff}}^2 \equiv -2\ln(\mathcal{L}^P(\varphi_{\text{max}}) - \mathcal{L}^P(\varphi)) < 1$ with the 68% confidence interval. We note that this interval may not have the desired frequentist coverage properties if the profile likelihood is not Gaussian [16].

2.4 Construction of the profile likelihood

We construct the marginalised posteriors from Markov chains generated with a modified version of the public Markov chain Monte Carlo sampler CosmoMC [17], using a conservative Gelman-Rubin convergence criterion [18] of $R-1 < 0.01$, and making sure that the numerical precision settings are sufficient for the data sets considered.

Naïvely, one might think that one could use the same chains to construct the profile likelihood, by binning the data in N_{eff} and identifying the best-fitting point in each bin. Unfortunately, this method does not turn out to be suitable for the case at hand. The reason is that the standard Metropolis-Hastings algorithm samples the region near the maximum of the posterior very poorly. In Appendix A we present a rough analytical estimate of the probability of finding at least one sample of a Markov chain within a given $\Delta\chi_{\text{eff}}^2$ of the best-fit. As shown in the bottom panel of figure 4, for our 10-parameter model one would need of order 10^5 independent samples to even have a 50% chance of the best-fitting sample to lie within 0.5 of the true best-fit χ_{eff}^2 . This should be compared to the typically few times 10^4 correlated samples one usually has in Markov chains used for parameter estimation. The problem is exacerbated by the binning: in particular the estimate of \mathcal{L}^P for the bins in the tails of the marginalised posterior would be extremely inaccurate.

We therefore employ a different, numerically somewhat more demanding, construction that avoids under-sampling of the tails and is immune to biases introduced by a binning procedure. On a grid of fixed values of N_{eff} , we estimate the respective maxima of the likelihood by generating Markov chains at temperatures $T \ll 1$, with the temperature and length of chains chosen such that $\ln \mathcal{L}^P$ is estimated with an accuracy of at least 0.1. In addition, we determine the global best-fit by letting N_{eff} vary as well.

3 Results

In figure 1 we show the results for WMAP7+ACT data. Firstly, we note that the posteriors differ very little for the different priors, indicating a remarkable robustness of the results to the choice of prior. Secondly, the profile $\Delta\chi_{\text{eff}}^2$ clearly deviates from the parabolic shape one would expect for a Gaussian profile likelihood, showing an obvious skew towards the large- N_{eff} side, so we refrain from mapping it to frequentist confidence limits. Thirdly, \mathcal{L}^P is markedly shifted (by up to about two thirds of a standard deviation) towards lower values of N_{eff} compared to the marginalised posteriors. A similar tendency was also observed in [10], and, more recently, in [11] – however, their results for the same data set (both mode and likelihood ratio-based bounds) differ considerably from ours, possibly due to them attempting

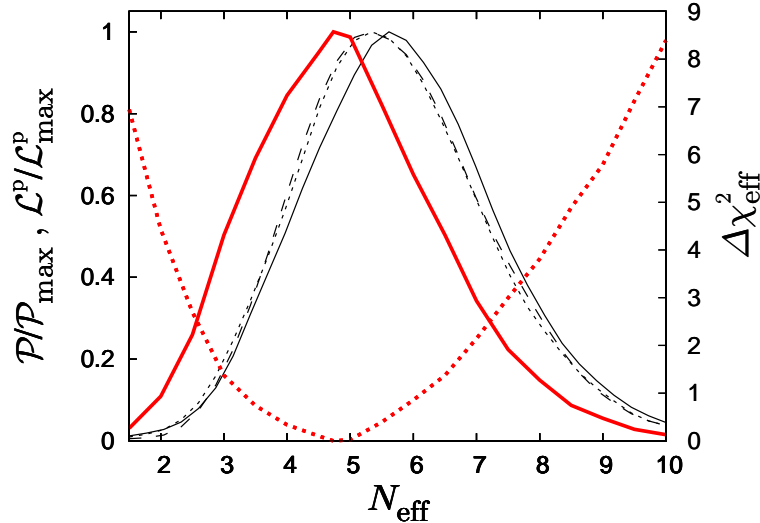


Figure 1. Constraints on N_{eff} from WMAP7+ACT data. Thin black lines denote the posterior probability density marginalised over the other parameter directions for three different choices of prior (solid: H_0 , dashed: θ_s , dotted: Ω_Λ). The profile likelihood is plotted in thick red lines, both in terms of $\mathcal{L}^p/\mathcal{L}_{\text{max}}^p$ (solid) and $\Delta\chi_{\text{eff}}^2$ (dotted).

to construct the profile likelihood from Markov chains that were originally generated for the purpose of Bayesian parameter inference. For instance, the individual best-fit estimates of the eight $T = 1$ WMAP+ACT Markov chains (each containing about 3×10^4 samples) we generated for constructing the marginalised posterior display a considerable spread, with a standard deviation of 0.57 – indicating the unreliability of this method.

Is there an explanation for why larger values of N_{eff} have a high posterior probability despite apparently not fitting the data too well (and *vice versa* for smaller N_{eff})? In [11], it was claimed that the effect, and, by association, also any possible hints for a deviation of N_{eff} from the standard model expectation, is “driven by prior effects”. This is a very generic statement however; it should be clear that any Bayesian credible intervals are always to some extent prior-dependent. We would like to propose a slightly more specific explanation here, namely that the shift of the marginalised posterior towards larger N_{eff} -enhancement is caused by a volume effect in the marginalisation process.

Let us, for a moment, imagine the full posterior were Gaussian. In that case, marginalisation and profiling would lead to the same result. Also, for a Gaussian posterior, the variance of the other parameters’ marginalised posteriors on slices of constant N_{eff} would not depend on N_{eff} . If, however, these variances did depend on N_{eff} , and happened to be positively correlated with N_{eff} , then at larger (smaller) N_{eff} there would be more (less) volume in the nuisance directions, and the marginalised posterior would be enhanced (suppressed) compared to the profile. We shall see that this is indeed the case here, and there is in fact a simple physical argument for why it should be so.

As discussed in [7, 19], N_{eff} impacts the CMB power spectra in several ways; most

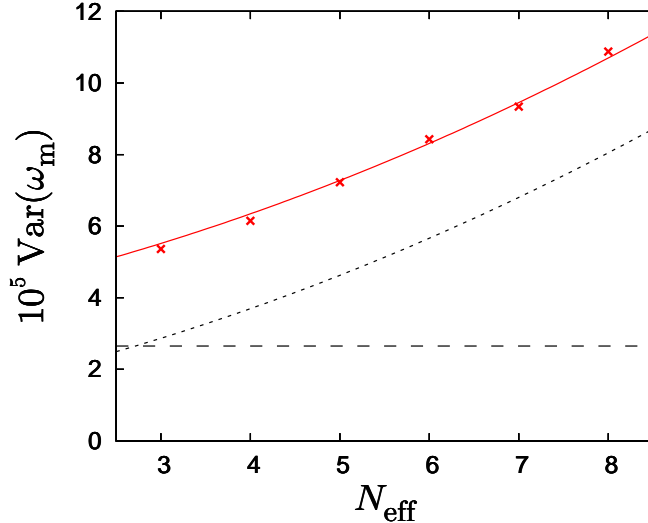


Figure 2. Variance of the marginalised posterior probability of ω_m on slices of width $\Delta N_{\text{eff}} = 1$ as a function of N_{eff} . The crosses mark the values extracted from the Markov chains, the red line is the prediction based on the variance of z_{eq} , consisting of a constant term induced by the bin width (equation (3.3), dashed line) and the intrinsic variance of ω_m (equation (3.2), dotted line).

importantly through the redshift of matter-radiation equality

$$1 + z_{\text{eq}} \equiv \frac{\rho_m}{\rho_r} = \frac{\omega_m}{\omega_\gamma} \frac{1}{1 + \alpha N_{\text{eff}}}, \quad (3.1)$$

which determines the magnitude of the early integrated Sachs-Wolfe effect. It is actually z_{eq} (not N_{eff} or the matter density ω_m) that is *directly* constrained by the CMB [20], and hence essentially uncorrelated with ω_m and N_{eff} . Ignoring the tiny uncertainty in the photon energy density ω_γ , the variance of ω_m for fixed N_{eff} is given by

$$\text{Var}(\omega_m)|_{N_{\text{eff}}} \simeq \text{Var}(z_{\text{eq}}) (\omega_\gamma (1 + \alpha N_{\text{eff}}))^2, \quad (3.2)$$

and thus the posterior becomes wider in the ω_m -direction for larger N_{eff} . Since ω_m has degeneracies with other parameters, such as H_0 , the widening is propagated to those directions as well, amplifying the total volume effect. In figure 2 we show the N_{eff} -dependence of the posterior’s width: using our original Markov chains, we evaluate the variance of the marginalised posterior of ω_m on slices of width $\delta N_{\text{eff}} = 1$. This is compared to the expectation from the measurement of $z_{\text{eq}} = 3180 \pm 129$, which can easily be calculated from the same chains. The variance on these slices is composed of two components, the intrinsic one of equation (3.2), and a constant piece due to the bin width, given by

$$\text{Var}_b(\omega_m) = \frac{1}{12} \omega_\gamma^2 z_{\text{eq}}^2 \alpha^2 \delta N_{\text{eff}}^2. \quad (3.3)$$

Their sum is found to be in excellent agreement with the variances from the chains.

The constraints on N_{eff} can be improved by adding non-CMB data to break some of the parameter degeneracies, and most of the recent hints for $N_{\text{eff}} > 3.046$ are based on such

combinations of data. As an example, we add the HST-constraint on H_0 here, which breaks the $N_{\text{eff}}-H_0$ degeneracy. Our results for WMAP7+ACT+HST data are shown in figure 3. The profile likelihood is closer to Gaussian now, and the magnitude of the volume effect has become much smaller – \mathcal{L}^{P} is shifted by roughly 0.2 with respect to the marginalised posteriors. If we compare this to the posterior standard deviation of ~ 0.7 , we see that the volume effect by itself cannot account for the observed deviation from the standard model expectation. We summarise our results in table 2.

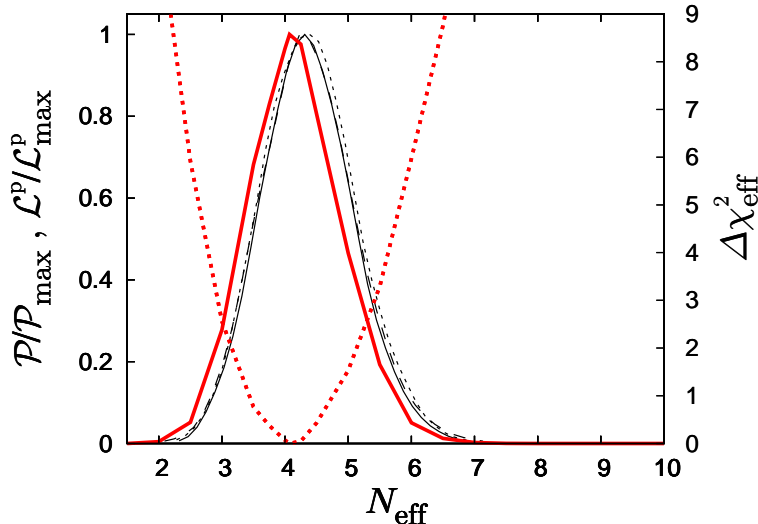


Figure 3. Same as figure 1, for WMAP7+ACT+HST.

Table 2. Summary of constraints on N_{eff} from different analysis methods. For the marginalised posterior we list the mean $\langle N_{\text{eff}} \rangle$, mode \mathcal{P}_{max} , standard deviation $\sigma_{N_{\text{eff}}}$, and the minimal 68%- and 95%-credible intervals [10]. For the profile likelihood, we list the mode $\mathcal{L}_{\text{max}}^{\text{P}}$ and the intervals in which $\Delta\chi_{\text{eff}}^2 \leq 1$ and 4, respectively.

Analysis	WMAP7+ACT					WMAP7+ACT+HST				
	$\langle N_{\text{eff}} \rangle$	\mathcal{P}_{max}	$\sigma_{N_{\text{eff}}}$	68% MCI	95% MCI	$\langle N_{\text{eff}} \rangle$	\mathcal{P}_{max}	$\sigma_{N_{\text{eff}}}$	68% MCI	95% MCI
H_0 -prior	5.78	5.68	1.45	4.18→7.12	3.03→8.76	4.37	4.30	0.72	3.61→5.03	2.96→5.80
θ_s -prior	5.69	5.20	1.44	4.02→6.92	3.01→8.59	4.37	4.28	0.75	3.57→5.05	2.89→5.86
Ω_Λ -prior	5.67	5.20	1.46	4.05→6.98	2.90→8.65	4.39	4.28	0.74	3.60→5.08	2.98→5.89
Profile		$\mathcal{L}_{\text{max}}^{\text{P}}$		$\Delta\chi_{\text{eff}}^2 \leq 1$	$\Delta\chi_{\text{eff}}^2 \leq 4$		$\mathcal{L}_{\text{max}}^{\text{P}}$		$\Delta\chi_{\text{eff}}^2 \leq 1$	$\Delta\chi_{\text{eff}}^2 \leq 4$
\mathcal{L}^{P}		4.73		3.29→6.14	2.12→8.09		4.07		3.43→4.76	2.79→5.50

4 Discussion

We have demonstrated that constraints on the effective number of neutrino species, inferred from CMB data, can be subject to a slight discrepancy between the Bayesian marginalised posterior and the profile likelihood. This can be attributed to a volume effect primarily in the ω_m direction, caused by the fact that the CMB data are directly sensitive mostly to the redshift of equality, not N_{eff} itself.

Before we come to an interpretation, let us illuminate the statistical aspect of this result. Regarded from a sampling theory perspective, the mode of the full multi-dimensional posterior can be regarded as an unbiased estimator of the true parameter values (since in the present problem it coincides by construction with the maximum of the likelihood). In the process of marginalisation, this property is lost – the most probable value of N_{eff} does not provide the best possible fit to the data, or, in other words, the mode of $\mathcal{P}(N_{\text{eff}})$ becomes a biased estimator of N_{eff} (see also [21] for a discussion, or [22] for another applied example). The profile likelihood on the other hand retains the unbiasedness of the mode estimator, but, unlike the marginalised posterior, it is not sensitive to volume effects, and thus does not have a formal statistical interpretation.

In general it should not come as a surprise that, whenever the full posterior/likelihood’s dimensionality is reduced, loss of information will be incurred. Marginalisation and profiling simply preserve different properties of their related multi-dimensional objects, and can thus be a good diagnostic of unusual features. A discrepancy between the two would point to a deviation from Gaussianity, and, from a Bayesian perspective, could for instance indicate that a certain amount of fine-tuning relative to the prior expectation is required in order to optimise the fit to the data.¹

Finally, to evaluate the relevance of this effect, the magnitude of the bias should be set in relation to the intrinsic width of the marginal distribution. For WMAP+ACT data, the difference between profile and posterior is of order two thirds of a standard deviation, thus not contributing the dominant – but certainly a non-negligible – part to the indication for a non-standard N_{eff} . With the addition of HST data, however, the bias is reduced to less than one third of a standard deviation, and a similar trend is to be expected if one added, for instance, large scale structure data, or improved measurements of the CMB damping tail – be it existing ones from the South Pole Telescope [5], or upcoming ones from Planck.

We conclude that the recent indication for a deviation of N_{eff} from its standard model expectation cannot be accounted for by this statistical effect alone (though the presence of an additional statistical bias introduced, e.g., by the modelling of foregrounds, remains a possibility).

Acknowledgements

The author thanks Steen Hannestad and Yvonne Wong for helpful comments on the manuscript and gratefully acknowledges support from a Feodor Lynen-fellowship of the Alexander von Humboldt Foundation and the use of computing resources from the Danish Center for Scientific Computing (DCSC).

¹We remark that one could, in principle, choose the priors such that the discrepancy would vanish (e.g., here, a flat prior on z_{eq} instead of N_{eff} might be a good guess). But with N_{eff} arguably being a more fundamental quantity than z_{eq} , it is doubtful whether such a choice could be reasonably justified from a theoretical point of view.

References

- [1] D. J. Fixsen, *Astrophys. J.* **707** (2009) 916-920, [arXiv:0911.1955].
- [2] G. Mangano, G. Miele, S. Pastor, T. Pinto, O. Pisanti, P. D. Serpico, *Nucl. Phys.* **B729** (2005) 221-234, [hep-ph/0506164].
- [3] J. Hamann, S. Hannestad, G. G. Raffelt, I. Tamborra and Y. Y. Y. Wong, *Phys. Rev. Lett.* **105** (2010) 181301, [arXiv:1006.5276].
- [4] E. Giusarma, M. Corsi, M. Archidiacono, R. de Putter, A. Melchiorri, O. Mena and S. Pandolfi, *Phys. Rev.* **D83** (2011) 115023. [arXiv:1102.4774].
- [5] R. Keisler *et al.*, *Astrophys. J.* **743** (2011) 28, [arXiv:1105.3182].
- [6] T. L. Smith, S. Das and O. Zahn, *Phys. Rev. D* **85** (2012) 023001, [arXiv:1105.3246].
- [7] Z. Hou, R. Keisler, L. Knox, M. Millea, C. Reichardt, [arXiv:1104.2333].
- [8] J. Hamann, S. Hannestad, G. G. Raffelt, Y. Y. Y. Wong, *JCAP* **1109** (2011) 034, [arXiv:1108.4136].
- [9] M. Archidiacono, E. Calabrese and A. Melchiorri, *Phys. Rev. D* **84** (2011) 123008, [arXiv:1109.2767].
- [10] J. Hamann, S. Hannestad, G. G. Raffelt, Y. Y. Y. Wong, *JCAP* **0708** (2007) 021. [arXiv:0705.0440].
- [11] A. X. Gonzalez-Morales, R. Poltis, B. D. Sherwin and L. Verde, [arXiv:1106.5052].
- [12] E. Komatsu *et al.* (WMAP Collaboration), *Astrophys. J. Suppl.* **192** (2011) 18, [arXiv:1001.4538].
- [13] J. Dunkley *et al.*, *Astrophys. J.* **739** (2011) 52, [arXiv:1009.0866].
- [14] A. G. Riess *et al.*, *Astrophys. J.* **730** (2011) 119, [arXiv:1103.2976].
- [15] W. Valkenburg, J. Hamann, L. M. Krauss, *Phys. Rev.* **D78** (2008) 063521, [arXiv:0804.3390].
- [16] F. Porter, *Nucl. Instrum. Meth.* **A368** (1996) 793-803.
- [17] A. Lewis and S. Bridle, *Phys. Rev. D* **66** (2002) 103511, [astro-ph/0205436].
- [18] A. Gelman, D. B. Rubin, *Statist. Sci.* **7** (1992) 457-472.
- [19] S. Bashinsky, U. Seljak, *Phys. Rev.* **D69** (2004) 083002, [astro-ph/0310198].
- [20] E. Komatsu *et al.* (WMAP Collaboration), *Astrophys. J. Suppl.* **180** (2009) 330-376, [arXiv:0803.0547].
- [21] J. Lesgourgues and S. Pastor, *Phys. Rept.* **429** (2006) 307, [astro-ph/0603494].
- [22] R. Stompor, S. M. Leach, F. Stivoli and C. Baccigalupi, *Mon. Not. Roy. Astron. Soc.* **392** (2009) 216, [arXiv:0804.2645].

A Profiling with Markov chains

In this section we present an estimate of how well the maximum of a probability distribution can be determined by using a Markov chain of length N .

Let \mathcal{P} be a probability distribution on an n -dimensional parameter space \mathfrak{P} , and $\varphi \in \mathfrak{P}$ be a point in this parameter space. We shall make two simplifying assumptions at this point: first, $\mathcal{P}(\varphi)$ can be approximated by an n -variate Gaussian distribution, and second, all the samples in the chain are independent. Without loss of generality one can then take $\mathcal{P}(\varphi)$ to have unit variance and be centered around $\varphi_{\max} = \vec{0}$. Define

$$\Delta\chi_{\text{eff}}^2(\varphi) \equiv -2(\ln \mathcal{P}(\varphi_{\max}) - \ln \mathcal{P}(\varphi)), \quad (\text{A.1})$$

and the volume fraction f_x of \mathcal{P} for which $\Delta\chi_{\text{eff}}^2(\varphi) < x$,

$$f_x = \int_{V_x} d\varphi \mathcal{P}(\varphi), \quad (\text{A.2})$$

with the volume V_x implicitly given by the condition $\varphi \in V_x \Leftrightarrow \chi_{\text{eff}}^2(\varphi) < x$. If one expresses φ in spherical coordinates, it can easily be shown that

$$f_x(n) = \int_0^{\sqrt{x}} dr \frac{1}{(\sqrt{2\pi})^{n/2}} \exp\left[-\frac{r^2}{2}\right] r^{n-1} \frac{(2\pi)^{n/2}}{\Gamma\left(\frac{n}{2}\right)}, \quad (\text{A.3})$$

where Γ is the Gamma function. If, instead of sampling from \mathcal{P} , one generates the Markov chain with a temperature parameter T by sampling from $\mathcal{P}^{1/T}$, equation (A.3) can be generalised to

$$f_x(n, T) = \int_0^{\sqrt{x}} dr \frac{T^{-n/2}}{(\sqrt{2\pi})^{n/2}} \left(\exp\left[-\frac{r^2}{2}\right]\right)^{1/T} r^{n-1} \frac{(2\pi)^{n/2}}{\Gamma\left(\frac{n}{2}\right)}. \quad (\text{A.4})$$

If all N samples of the chain are independent, then the probability \bar{p} that none of the points lie within f_x is given by

$$\bar{p}(x, n, T, N) = (1 - f_x(n, T))^N. \quad (\text{A.5})$$

It follows trivially that the probability of at least one point of the chain being within $\Delta\chi_{\text{eff}}^2 = x$ of $\chi_{\text{eff}}^2(\varphi_{\max})$ is $p(x, n, T, N) \equiv 1 - \bar{p}(x, n, T, N)$. For a few selected slices in (n, T, N) -space, $p(x, n, T, N)$ is plotted in figure 4.

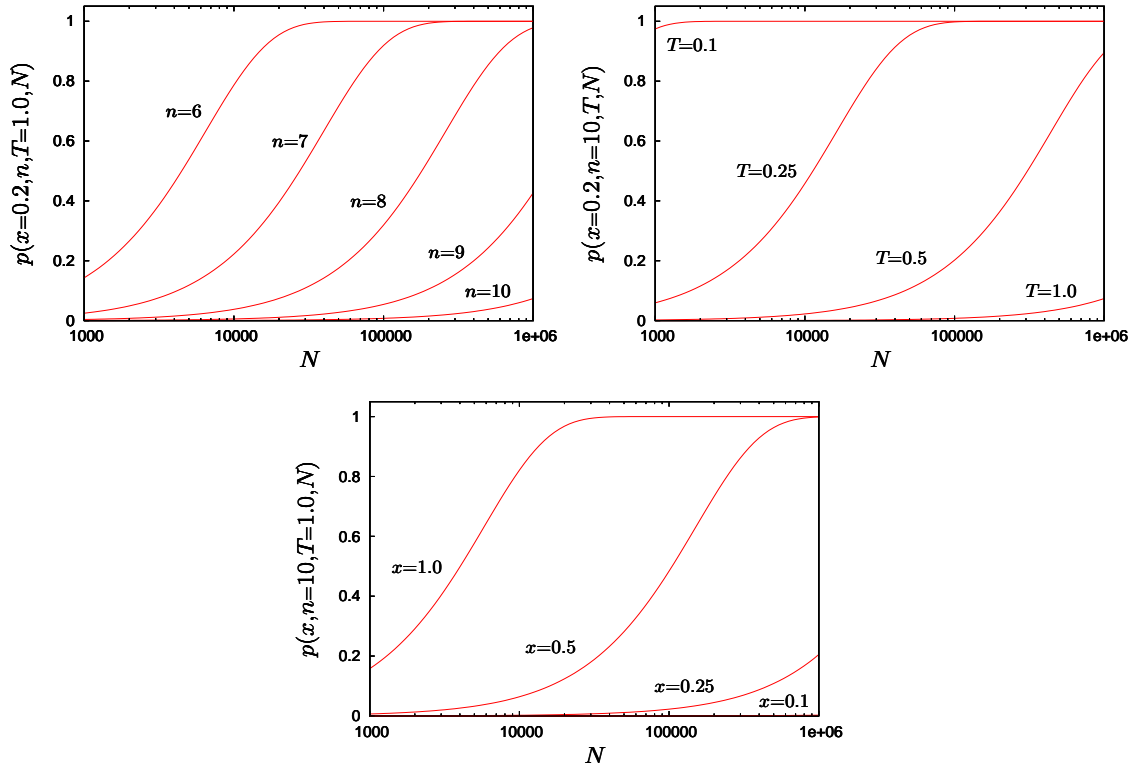


Figure 4. Probability of finding at least one sample within $\Delta\chi_{\text{eff}}^2 = x$ of the true maximum of the n -dimensional Gaussian posterior \mathcal{P} , if the Markov chain was generated at a temperature T and contains N independent samples. *Top left:* dependence on N and n for $T = 1$ and $x = 0.2$. *Top right:* dependence on N and T for $n = 10$ and $x = 0.2$. *Bottom:* dependence on N and x for $T = 1$ and $n = 10$.